International Journal of Microwave and Wireless Technologies, 2017, 9(10), 1951–1960. © Cambridge University Press and the European Microwave Association, 2017
doi:10.1017/S1759078717000952

RESEARCH PAPER

Design of dual/tri-frequency impedance transformer with ultra-high transforming ratio

RUSAN KUMAR BARIK AND S. S. KARTHIKEYAN

In this article, the design of a new dual-band impedance transformer with ultra-high transforming ratio (UHTR) is presented. The closed-form expressions are derived analytically using a lossless transmission-line theory. To practically validate the proposed design concept, two examples of dual-band transformer working at smaller and larger frequency ratios are designed for different load impedance of 500, 1000, and 1500 Ω. Finally, three prototypes of dual-band transformer with UHTR are designed, fabricated, and tested. For all these prototypes, different frequency ratios (two operating frequencies can be chosen arbitrarily) are considered. The measured return loss of the prototypes is better than 15 dB at all the operating frequencies. The measured results are matched very closely with the simulated results. This design is then extended to match a complex load at two different frequencies. The multi-band characteristic is obtained by decomposing a shorted stub into a stepped impedance section of the proposed structure. With the necessary derivation and analysis, a tri-frequency matching network is designed for a transforming ratio of 10.

Keywords: Passive components and circuits, Computer-aided design, Modeling, Simulation and characterizations of devices and circuits

Received 24 March 2017; Revised 7 August 2017; Accepted 16 August 2017; first published online 29 September 2017

I. INTRODUCTION

Impedance transformer (IT) is one of the basic elements employed for the design of many radiofrequency (RF)/microwave systems. The main aim of the IT/matching network is to minimize the reflection between the connected circuits. In addition, it provides advantages such as maximum power transfer, high linearity, and low noise level. Therefore, IT finds large applications in antenna feed lines, mixers, microwave amplifiers, power dividers, etc. The conventional $\lambda/4$ microstrip line has been extensively used, but it can only be operated at single frequency and difficult in implementation for large load impedances. To compete with advanced communication system with multi-standard applications, it is essential to convert a single-frequency IT to a multi-frequency IT. Therefore, the design of multi-band ITs (MBITs) with ultra-high transforming ratio (UHTR) become unique challenge for many researchers. The particular use of multi-band matching network with UHTR can be found in the design of multi-band power amplifier and rectenna. In the case of rectenna design for RF energy harvesting application, the real-part of input impedance of diode for rectification could be very high (>400 Ω), especially at lower input powers [1, 2]. Hence, this high input impedance should be matched to a real source of 50 Ω. Furthermore, in any high-frequency power-amplifier design, improper impedance matching will degrade the stability and reduce the circuit efficiency. In multi-band amplifier design, this consideration is even more critical. The problem occurs because the resonated impedance may be more than 500 Ω and reducing this to 50 Ω is a key challenge (http://www.nxp.com/products/rf/rf-amplifiers-low-medium-power:MC_50961; https://www.minicircuits.com/WebStore/Transformers.html). Hence, the design of dual-band matching network with UHTR has a great demand in the wireless industry today.

To surpass these issues, several dual-band ITs (DBITs) are developed for real as well as complex loads [3–11]. To deal with the frequency-dependent complex loads, DBITs have been designed employing two-section shunt stubs [3], *T*-type network [4], π-model [5], *T*-shaped coupled line [6], transmission line with shunt stubs [7], coupled line with open/short stub [8], *T*-network, [9] and π/*T*-type network [10]. The DBITs based on the two-section transmission line [11–14] are used to match real loads with 50 Ω source. Many transformers are designed to operate at single frequency for small [15, 16] and large load impedances [17–23]. An IT with transforming ratio of 3.4 has been developed by employing coupled three-line [17]. In [18], a coupled line has been used to design an IT with transforming ratio of 3.4. The modified coupled-line IT has been reported for a transforming ratio

Indian Institute of Information Technology Design & Manufacturing Kancheepuram, Chennai 600127, India
Corresponding author:
R. K. Barik
Email: edm15d003@iiitdm.ac.in

https://doi.org/10.1017/S1759078717000952 Published online by Cambridge University Press

of 5 in [19]. A broadband IT [20] has been demonstrated for an impedance transforming ratio of 5. A wideband IT with transforming ratio of 5 has been developed using coupled line and open-ended stub [21]. In [22], a coupled-line IT with bandpass characteristic has been designed. Two and three sections short-ended coupled lines have been employed to develop a wideband IT for UHTR of 20 in [23]. Recently, two quad-band matching networks have been developed for UHTR [24, 25]. To meet the present day demand for wireless systems on design of multi-band devices, it is necessary to transfer single-band IT to MBIT for large source/load impedances.

In this paper, the design of ultra-high transforming DBIT is presented. Our main effort to match large real loads to a 50 Ω source at two different frequencies. The design equations are derived analytically to obtain the dual-band operation. To validate the proposed topology, three types of DBIT with different transforming ratios of 10, 20, and 30 are designed, fabricated, and tested. To prove the flexibility of the proposed transformer, different frequency ratios (two operating frequencies can be chosen arbitrarily) are considered for all the examples. The measured return loss is better than 15 dB at each operating frequency. Furthermore, the proposed idea for matching a complex load at two different operating frequencies is validated numerically. In addition, a tri-band matching network (TBMN) for UHTR is obtained by adding a stepped impedance section to the proposed structure.

II. ANALYSIS OF THE PROPOSED DBIT

As depicted in Fig. 1, the dual-band topology consists of two series transmission lines (Z_R, θ_R) with two short-ended stubs (Z_S, θ_S) shunted at the center. The S-parameters of the proposed dual-band network can be computed as equation (1), from the ABCD parameters:

$$S_{11} = \frac{rZ_L A_o + r^2 B_o - Z_L^2 C_o - rZ_L D_o}{rZ_L A_o + r^2 B_o + Z_L^2 C_o + rZ_L D_o}, \tag{1a}$$

$$S_{21} = \frac{2rZ_L}{rZ_L A_o + r^2 B_o + Z_L^2 C_o + rZ_L D_o}, \tag{1b}$$

$$\angle S_{21} = -\frac{\pi}{2} + \tan^{-1}\left[\frac{2rZ_L A_o B_o}{r^2 B_o^2 + Z_L^2 - Z_L^2 A_o^2}\right], \tag{1c}$$

$$A_o = D_o = \cos^2\theta_R - 2B_S Z_R \sin\theta_R \cos\theta_R - \sin^2\theta_R, \tag{2a}$$

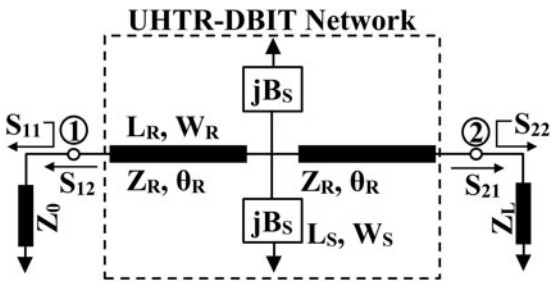

Fig. 1. Schematic representation of the proposed dual-band impedance transformer.

$$B_o = jZ_R \sin\theta_R \cos\theta_R - jB_S Z_R^2 \sin^2\theta_R, \tag{2b}$$

$$C_o = j\frac{2\sin\theta_R \cos\theta_R}{Z_R} + jB_S \cos^2\theta_R, \tag{2c}$$

$$r = \frac{Z_L}{Z_o}. \tag{3}$$

And the electrical lengths of the proposed network can be written as:

$$\theta_R = \frac{n_1 \pi f_1}{f_1 + f_2}, \tag{4}$$

$$\theta_S = \frac{n_2 \pi f_1}{f_1 + f_2}. \tag{5}$$

Here n_1 and n_2 are integers.

As the proposed topology is made equivalent to a λ/4 transmission line having characteristic impedance of $\sqrt{r}Z_o$, $\angle S_{21}$ is set to 90°, the numerator of equation (1c) should be zero and reduced to $A_o = 0$, which implies:

$$B_S = \frac{\cos 2\theta_R}{Z_R \sin 2\theta_R}, \tag{6}$$

$$Z_S = -\frac{\sqrt{r}Z_o \tan 2\theta_R \tan\theta_S}{\tan\theta_R}. \tag{7}$$

To obtain the dual-band operation, the proposed structure should satisfy another condition, which is given as:

$$B_o = j\sqrt{r}Z_o = jZ_{eq}. \tag{8}$$

Solving equations (2b) and (8), we get

$$Z_R = \frac{\sqrt{r}Z_o}{\tan\theta_R}. \tag{9}$$

In order to design a UHTR-DBIT, a simple synthesis approach is summarized as follows:

(1) Select the source (Z_o) and load (Z_L) impedances. For $Z_o = 50\Omega$, $Z_{eq} = 50\sqrt{r}\Omega$, where $r = Z_L/Z_o$.
(2) Choose two operating frequencies f_1 and f_2, then compute the electrical lengths θ_R and θ_S using the equations (4) and (5), respectively, by choosing appropriate values of n_1 and n_2.
(3) For compactness, the value of n_2 is chosen as 1.The smaller and larger frequency ratios can be obtained by selecting $n_1 = 1$ and $n_1 = 2$, respectively.
(4) The characteristic impedances Z_S and Z_R can be obtained from the equations (7) and (9), respectively.
(5) Check whether the calculated values of Z_S and Z_R can be realizable in microstrip technology. If it is unrealizable, go back to step 2 and increase the values of n_1 and n_2.
(6) The physical parameters of the proposed network can be evaluated at the first operating frequency f_1.

https://doi.org/10.1017/S1759078717000952 Published online by Cambridge University Press

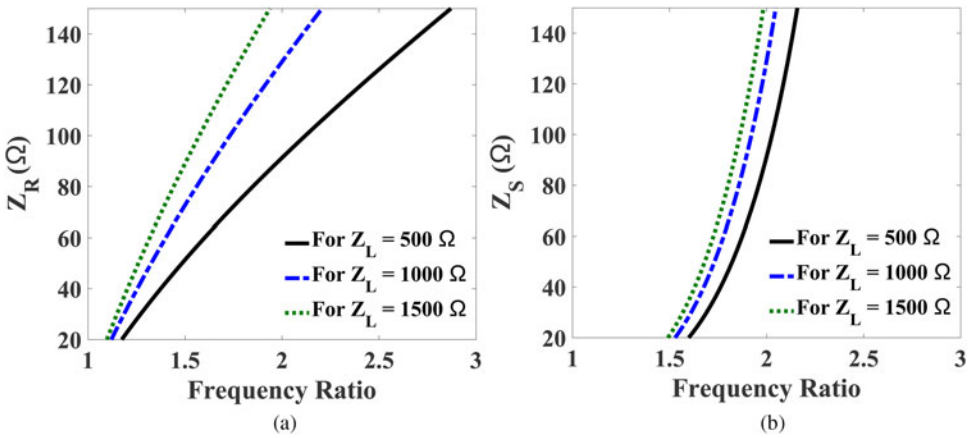

Fig. 2. The impedance values of the proposed DBIT for different load (Z_L). (a) Plot of Z_R versus smaller frequency ratios (f_2/f_1) and (b) plot of Z_S versus smaller frequency ratios (f_2/f_1).

To design dual-band microwave components for all commercial dual-band applications, it is essential for a technique to provide smaller as well as larger frequency ratios, in which most of the popular wireless standards such as GSM, GPRS, WiMAX, WLAN, and Bluetooth can be covered. To calculate the realizable frequency ratios of the proposed UHTR-DBIT, the transcendental equations (7) and (9) are solved graphically for different load impedance values (Z_L). Figure 2 illustrates the impedance values Z_R and Z_S for smaller frequency band ratios. Similarly, the impedance values Z_R and Z_S for larger frequency band ratios are plotted in Fig. 3. We considered 0.8 thick FR4 substrate having dielectric constant of 4.4 for all these calculations. This implies the limitation of impedance values for microstrip technology is 20–120 Ω. For a transforming ratio of 10, i.e. $Z_L = 500\ \Omega$, the smaller and larger frequency ratios obtained from Figs 2 and 3 are 1.6–2.08 and 3.64–4.45, respectively. The calculated frequency band ratios for different load impedance values are depicted in Table 1. From the table, it is observed that the proposed UHTR-DBIT is suitable for many popular communication standards and feasible for inclusion in most of the RF/microwave systems design. Table 2 depicts the design parameters required to implement a DBIT with transforming ratio of 10 and frequency band ratio of 2 for the proposed unit and previously reported schematics. As seen in Table 2, the impedance values are beyond the practical realization limits of the microstrip technology. Therefore, the topologies reported in [6–10] are not suitable for UHTR. Hence, we proposed a new DBIT and its mathematical modeling to obtained the larger transforming ratio.

III. DESIGN OF THE UHTR-DBIT

In this section, two examples of UHTR-DBITs for smaller and larger frequency band ratios are designed and simulated to validate the proposed idea presented in the above section. Specifically, the load impedances of 500 Ω ($r = 10$), 1000 Ω ($r = 20$), and 1500 Ω ($r = 30$) are considered to match a source impedance of 50 Ω. Based on the closed form equations, the design parameters of the proposed DBIT with different transforming ratios for smaller and larger frequency band ratios are computed and listed in Table 3. Theoretically calculated S_{11} of the DBIT for smaller and larger frequency band ratios (f_2/f_1) are depicted in Fig. 4. The calculated S_{11} is well below −20 dB, which proves good matching between source and load impedances at the two arbitrary frequencies. Furthermore, the bandwidth of a DBIT is a crucial parameter that needs to be focused. In the design of dual-band RF systems, it is necessary to produce significant amount of bandwidth for practical applications. In practice, the bandwidth of the transformer increases/decreases for less mismatched load (as Z_L becomes closer to Z_o) and more mismatched load (as Z_L becomes far to Z_o), respectively [26]. Hence, the behavior

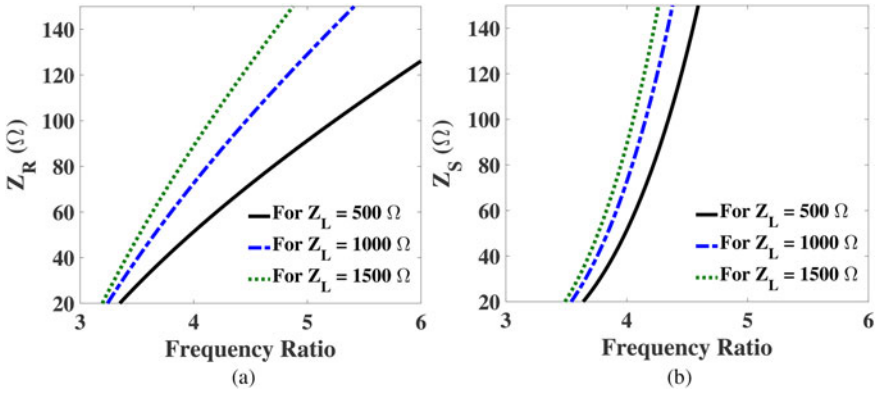

Fig. 3. The impedance values of the proposed DBIT for different load (Z_L). (a) Plot of Z_R versus larger frequency ratios (f_2/f_1) and (b) plot of Z_S versus larger frequency ratios (f_2/f_1).

https://doi.org/10.1017/S1759078717000952 Published online by Cambridge University Press

Table 1. Calculation of the realizable frequency band ratios.

Load impedances	Smaller frequency band ratios	Larger frequency band ratios
$Z_L = 500\ \Omega$	1.6–2.08	3.64–4.450
$Z_L = 1000\ \Omega$	1.53–1.97	3.55–4.25
$Z_L = 1500\ \Omega$	1.5–1.71	3.49–4.41

of the load in the design of the proposed dual-band transformer is illustrated in Fig. 4. From the figure, It is observed that the bandwidth decreases with increasing load. It is also seen that the bandwidth is more than 100 MHz (considering $S_{11} < -10$ dB), which is suitable for most of the application. Therefore, the proposed DBIT provides flexible solutions for implementation of very large impedance transforming ratio and can be applied to design microwave devices, such as amplifiers, power dividers, and antennas.

IV. DUAL-BAND MATCHING NETWORK FOR A COMPLEX LOAD $(R_1 + jX_1)$

The proposed analysis is applicable for a complex load impedance by adding one transmission line to the DBIT network as shown in Fig. 5. In the above section, we have discussed the design of dual-frequency IT for real load impedances. Therefore, this section extends the application scope of dual-band matching network for a complex load impedance. In order to validate numerically, we have considered a complex impedance of $Z_L = R_1 + jX_1\Omega$ to match with the source impedance of 50 Ω. The design of DBIT for complex load consists of two steps. Firstly, a transmission line with characteristic impedance of Z_a and electrical length of θ_a is used to convert the complex load into a real impedance of Z_c as shown in stage I of Fig. 5. Finally, the real value is transformed by the proposed dual-band matching network. The closed form design formulas for stage I can be written as:

$$\theta_a = \tan^{-1}\left[\frac{\sqrt{4+\left(\frac{U}{Z_aX_1}\right)^2} \pm \frac{U}{Z_aX_1}}{2}\right], \tag{10}$$

$$Z_c = \frac{R_1^2 + (X_1 + Z_a\tan\theta_a)^2}{R_1(1+\tan^2\theta_a)}. \tag{11}$$

where

$$U = R_1^2 - Z_a^2 + X_1^2.$$

For a given value of $Z_L = R_1 + jX_1$ and assuming the realizable value of Z_a, the value of θ_a and Z_c can be computed from

Table 3. Design parameters of the proposed UHTR-DBIT for smaller and larger frequency ratios.

Designs	f_1/f_2 (GHz)	Z_L (Ω)	Z_R (Ω)	θ_R (°)	Z_S (Ω)	θ_S (°)
Figure 4a	1.5/2.4	500	59.96	69.23	20.14	69.23
		1000	84.8	69.23	28.5	69.23
		1500	103.86	69.23	34.9	69.23
Figure 4b	0.9/3.6	500	51.37	72	51.37	36
		1000	72.65	72	72.65	36
		1500	88.98	72	88.98	36

Table 2. Design parameters of the proposed unit and previously reported structures.

Ref	Techniques	Z_L/Z_o	f_2/f_1	Parameters values	Remarks
[10]	π-type	10	2	$Z_P = 182.5\ \Omega$, $Z_S = 182.5\ \Omega$, $\theta_P = 60^\circ$, $\theta_S = 120^\circ$	a, b
[11]	Two-section	10	2	$Z_1 = 232\ \Omega$, $Z_2 = 107.7\ \Omega$, $l_1 = 60^\circ$, $l_2 = 120^\circ$	a, b
[12]	Two-section transformer	10	2	$Z_1 = 111.8\ \Omega$, $Z_2 = 223.6\Omega$, $l_1 = 60^\circ$, $l_2 = 120^\circ$	a, b
[13]	Two-section transformer	10	2	$Z_1 = 111.8\ \Omega$, $Z_2 = 223.6\ \Omega$, $l_1 = 60^\circ$, $l_2 = 120^\circ$	a, b
[14]	Chebyshev transformer	10	2	$Z_1 = 111.8\ \Omega$, $Z_2 = 223.6\ \Omega$, $l_1 = 60^\circ$, $l_2 = 120^\circ$	a, b
This work	Transmission-line and stubs	10	2	$Z_P = 91.3\ \Omega$, $Z_S = 91.3\ \Omega$, $\theta_P = 60^\circ$, $\theta_S = 120^\circ$	C

a, The characteristic impedance values are beyond the realization limits of the microstrip technology; b, not suitable for UHTR; c, suitable for UHTR.

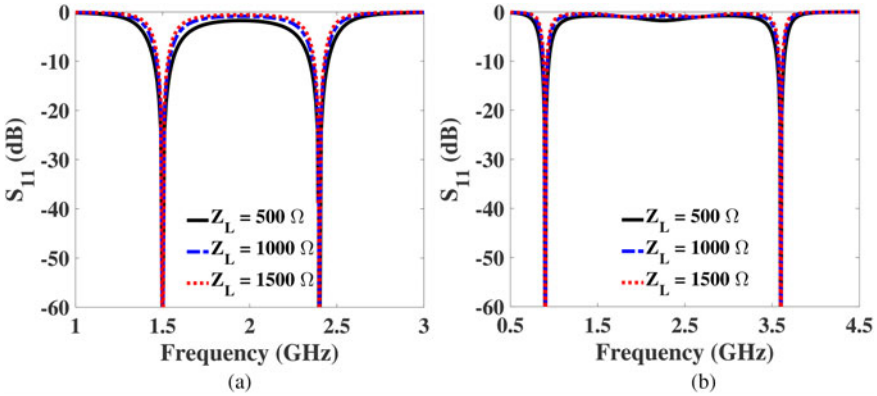

Fig. 4. Theoretically calculated S_{11} of the DBIT with transforming ratios of 10, 20, and 30. (a) For a smaller frequency band ratio of 1.6 and (b) for a larger frequency band ratio of 4.

https://doi.org/10.1017/S1759078717000952 Published online by Cambridge University Press

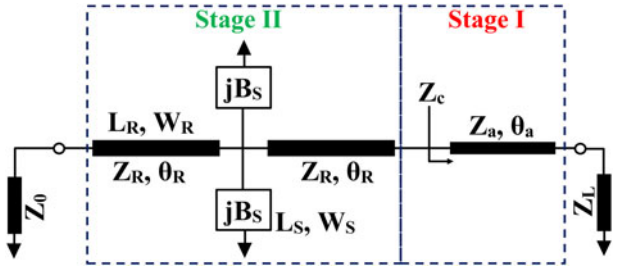

Fig. 5. Schematic layout of the proposed dual-band matching network for a complex load.

Table 4. Design parameters of the proposed DBIT for a complex load.

Z_L (Ω)	Z_o (Ω)	f_1/f_2 (GHz)	Z_R (Ω)	θ_R (°)	Z_S (Ω)	θ_S (°)	Z_S (Ω)	θ_S (°)
200 + j185.9	50	0.9/3.6	80.7	60	80.7	60	115	17.44

equations (10) and (11), respectively. As an example, the load impedance Z_L and the value of Z_a are considered as 200 + j185.9 and 115 Ω. The values of Z_c and θ_a are calculated as 390.73 Ω and 17.44°. For $Z_c = 390.73$ Ω, the value of Z_{eq} is computed as 139.77 Ω, and the corresponding design parameters of the dual-band matching network are listed in Table 4. Figure 6 presents the circuit simulated return loss performance of the dual-band transformer for a complex load. From the figure, it is seen that the return loss is more than 15 dB at each frequency band. Hence, the proposed dual-band design is also applicable for a complex load impedance.

V. DESIGN OF TRI-FREQUENCY MATCHING NETWORK

In this section, we have explored the multi-band characteristic of the proposed structure and designed a TBMN for a transforming ratio of 10. To obtain the tri-band operation, the proposed DBIT is slightly modified by decomposing a short circuited stub into a stepped impedance section as shown in Fig. 7. In the modified structure, the green-colored network

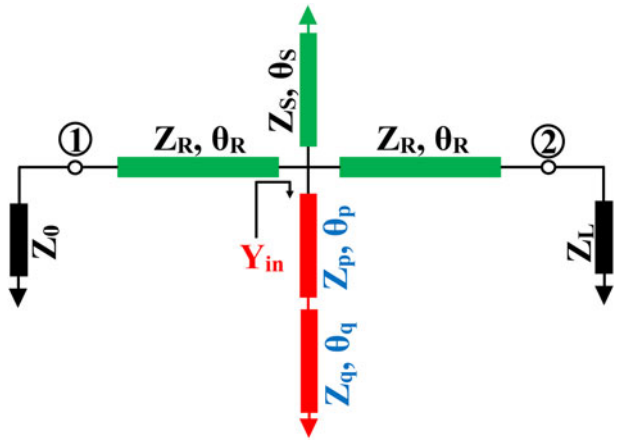

Fig. 7. Schematic representation of the proposed tri-band matching network.

Table 5. Design parameters of the proposed tri-frequency matching network.

$f_1/f_2/f_3$ (GHz)	Z_R (Ω)	θ_R (°)	Z_S (Ω)	θ_S (°)	Z_p (Ω)	θ_p (°)	Z_q (Ω)	θ_q (°)
1.5/3.45/6.45	112.6	54.54	115.8	54.54	47.7	54.4	24.2	54.54

is used to obtain dual-frequency operation (f_1 and f_2) and the stepped impedance structure (red-colored) is employed to achieve third operating frequency f_3. This stepped impedance will not meddling to the operating frequencies f_1 and f_2. Hence, the modified network is capable of producing tri-frequency characteristic. The analysis of the proposed TBMN is based on the following steps.

(a) To obtain dual-frequency operation, the design parameters of the green-colored structure are computed based on the procedure discussed in Section II.
(b) A detailed analysis is proposed to achieve third operating frequency (f_3).
(c) The design parameters of the red-colored network is derived in such a way that it will provide Z_{eq} at f_3 and infinity at two other frequencies (f_1 and f_2).

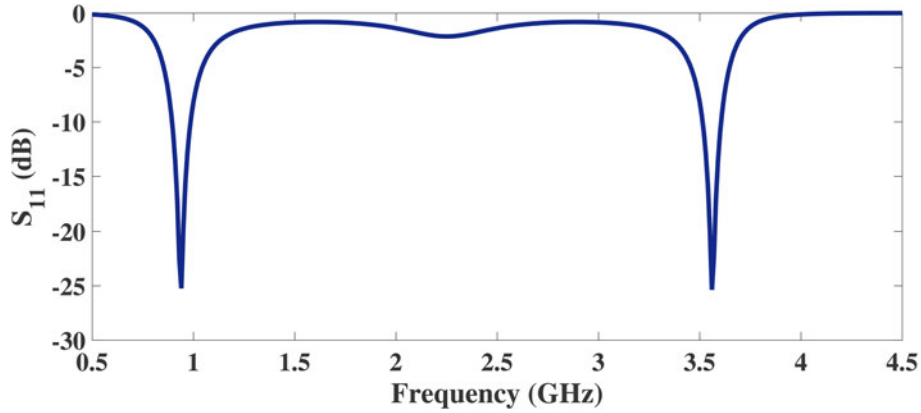

Fig. 6. Circuit simulated return loss of the proposed dual-band matching network for a complex load (200 + j185.9 Ω).

https://doi.org/10.1017/S1759078717000952 Published online by Cambridge University Press

Based on the synthesis procedure in Section II, the value of Z_p and Z_q are computed as:

$$Z_R = \frac{Z_{eq}}{\tan\theta_R}, \tag{12}$$

$$Z_S = -\frac{Z_R}{2}\tan 2\theta_R \cot\theta_S, \tag{13}$$

$$\theta_R = \theta_S = \frac{n\pi}{1+K_1}, \tag{14}$$

where

$$K_1 = \frac{f_2}{f_1}.$$

After achieving dual-frequency characteristic, the third operating frequency is obtained by employing the stepped impedance structure. This network is equivalent to a $\lambda/4$ transmission line (Z_{eq}) at f_3 without interrupting the dual-frequency characteristic of the green-colored structure. Thus, the desired TBMN will be obtained upon the satisfaction of these conditions. To validate the fact, the input admittance of the stepped impedance structure must be zero at f_1 and f_2, i.e.

$$Y_{in} = \frac{1}{Z_{in}} = j\frac{Z_q\tan\theta_q\tan\theta_p - Z_p}{Z_p^2\tan\theta_p + Z_pZ_q\tan\theta_q} = 0. \tag{15}$$

By solving equation (15), we get:

$$Z_p = Z_q\tan\theta_q\tan\theta_p, \tag{16}$$

where

$$\theta_p = \theta_q = \frac{n\pi}{1+K_1}.$$

To develop a relationship between f_2/f_1 and f_3, the overall ABCD matrix of the proposed TBMN structure is equated with a $\lambda/4$ transmission line with characteristic impedance of Z_{eq} as yield in equation (17).

$$\begin{bmatrix} A_t & B_t \\ C_t & D_t \end{bmatrix} = \begin{bmatrix} \cos\theta_R & jZ_R\sin\theta_R \\ j\frac{\sin\theta_R}{Z_R} & \cos\theta_R \end{bmatrix}\begin{bmatrix} 1 & 0 \\ -j\frac{\cot\theta_S}{Z_S} & 1 \end{bmatrix} \times \begin{bmatrix} 1 & 0 \\ j\frac{Z_q\tan\theta_q\tan\theta_p - Z_p}{Z_p^2\tan\theta_p + Z_pZ_q\tan\theta_q} & 1 \end{bmatrix}\begin{bmatrix} \cos\theta_R & jZ_R\sin\theta_R \\ j\frac{\sin\theta_R}{Z_R} & \cos\theta_R \end{bmatrix}. \tag{17}$$

From equation (17), we get:

$$A_t = \cos 2\theta_R - \frac{Z_R}{2}\sin 2\theta_R\left[-\frac{\cot\theta_S}{Z_S} + \frac{Z_q\tan\theta_q\tan\theta_p - Z_p}{Z_p^2\tan\theta_p + Z_pZ_q\tan\theta_q}\right], \tag{18}$$

$$B_t = jZ_R\sin 2\theta_R - Z_R^2\sin^2\theta_R\left[-\frac{\cot\theta_S}{Z_S} + \frac{Z_q\tan\theta_q\tan\theta_p - Z_p}{Z_p^2\tan\theta_p + Z_pZ_q\tan\theta_q}\right]. \tag{19}$$

Hence, by equating, $A_t = 0$ and $B_t = \pm jZ_{eq}$, the following equations are obtained:

$$\left[-\frac{\cot\theta_S}{Z_S} + \frac{Z_q\tan\theta_q\tan\theta_p - Z_p}{Z_p^2\tan\theta_p + Z_pZ_q\tan\theta_q}\right] = \frac{2\cot 2\theta_R}{Z_R}, \tag{20}$$

$$\left[-\frac{\cot\theta_S}{Z_S} + \frac{Z_q\tan\theta_q\tan\theta_p - Z_p}{Z_p^2\tan\theta_p + Z_pZ_q\tan\theta_q}\right] = \frac{Z_R\sin 2\theta_R - Z_{eq}}{Z_R^2\sin^2\theta_R}. \tag{21}$$

By solving equations (20) and (21), we can obtain:

$$\frac{2\cot(2K_2\theta_R)}{Z_R} = \frac{Z_R\sin(2K_2\theta_R) - Z_{eq}}{Z_R^2\sin^2(K_2\theta_R)}, \tag{22}$$

$$\frac{Z_q\tan(K_2\theta_q)\tan(K_2\theta_p) - Z_p}{Z_p^2\tan(K_2\theta_p) + Z_pZ_q\tan(K_2\theta_q)} = \frac{2\cot(2K_2\theta_R)}{Z_R} + \frac{\cot(K_2\theta_S)}{Z_S}, \tag{23}$$

$$\frac{Z_p}{Z_q} = \frac{\tan(K_2\theta_q)[\tan(K_2\theta_p) - LZ_p]}{LZ_p\tan(K_2\theta_p) + 1}, \tag{24}$$

where

$$K_2 = \frac{f_3}{f_1} \text{ and } L = \frac{2\cot(2K_2\theta_R)}{Z_R} + \frac{\cot(K_2\theta_S)}{Z_S}.$$

By solving equations (16) and (24), the values of Z_p and Z_q can be expressed as:

$$Z_p = \frac{\tan(K_2\theta_q)\tan(K_2\theta_p) - \tan\theta_q\tan\theta_p}{L[\tan(K_2\theta_p)\tan\theta_q\tan\theta_p + \tan(K_2\theta_q)]}, \tag{25}$$

$$Z_q = \frac{Z_p}{\tan\theta_q\tan\theta_p}. \tag{26}$$

https://doi.org/10.1017/S1759078717000952 Published online by Cambridge University Press

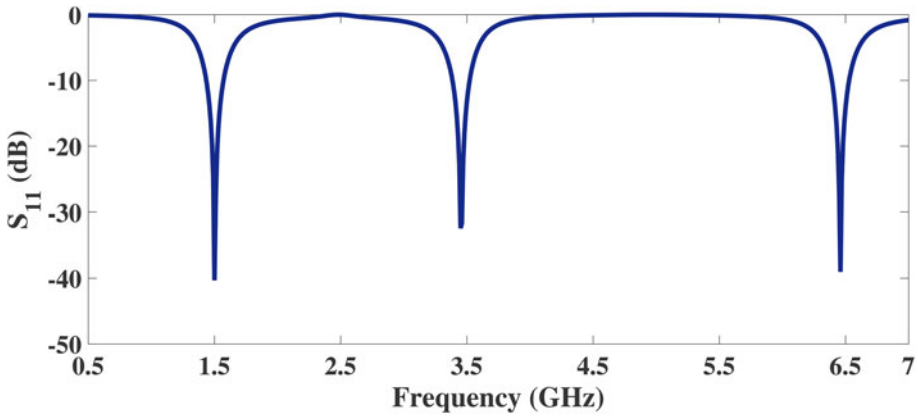

Fig. 8. Circuit simulated return loss of the proposed tri-band matching network for a transforming ratio of 10.

Table 6. Design parameters of the fabricated UHTR-DBITs.

Designs	f_1/f_2 (GHz)	Z_L (Ω)	Z_R (Ω)	θ_R (°)	Z_S (Ω)	θ_S (°)
DBIT I	1/2	500	91.3	60	91.3	60
DBIT II	3.5/5.8	1000	91.5	67.74	36.83	67.74
DBIT III	1.5/5.8	1500	78.67	73.97	65.4	36.98

Table 7. Physical dimensions of the fabricated UHTR-DBITs.

Designs	L_R (mm)	W_R (mm)	L_S (mm)	W_S (mm)
DBIT I	28.42	0.42	28.51	0.43
DBIT II	9.6	0.49	9	2.45
DBIT III	23.34	0.75	12.93	0.882

To design a TBMN, a systematic procedure is summarized as follows:

- Calculate the ratio K_1 by choosing two operating frequencies (f_2/f_1). Compute the values of Z_R, Z_S, θ_R, and θ_S using equations (12) and (13).
- Using equation (22), the value of K_2 ($=f_3/f_1$) is obtained.
- The values of Z_p and Z_q are computed using equations (25) and (26), respectively.

Initially, two operating frequencies are chosen for dual-band operation. For a load of 500 Ω, the realizable frequency ratio can be chosen between $1.76 < K_1 < 2.31$. After selection of two operating frequencies f_1 and f_2, the third operating frequency f_3 is calculated by using equation (22). For example, when $K_1 = 2.3$, the equality of the equation (22) is satisfied for the value of $K_2 = 4.3$. To validate the theoretical design process, a tri-band transformer operating at 1.5/3.45/6.45 GHz is designed and simulated. Based on the synthesis procedure, the design parameters are calculated for a transforming ratio of 10 ($Z_L =$ 500 Ω). For $Z_{eq} = \sqrt{r}Z_o = 158.11\ \Omega$, the parameter values are listed in Table 5. Figure 8 depicts the theoretical return loss of the TBMN for a transforming ratio of 10. From the figure, it is seen that the S_{11} is well below −20 dB at each frequency band. This implies the proposed network is capable of transferring a very high load to a source of 50 Ω at three different operating frequencies.

VI. FABRICATION AND MEASUREMENT

To support the circuit analysis, three DBITs with transforming ratios of 10, 20, and 30 are designed and fabricated. The load impedances $Z_L =$ 500, 1000, and 1500 Ω are considered to match a source impedance of 50 Ω and constructed by SMD resistors with the corresponding values. The design parameters of the UHTR-DBITs for transforming ratios of 10, 20, and 30 are computed and listed in Table 6. Based on

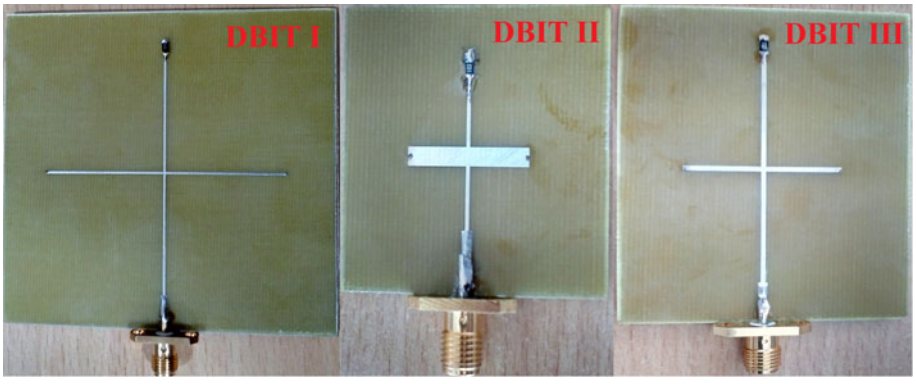

Fig. 9. Photograph of the fabricated UHTR-DBITs for real load impedances of $Z_L =$ 500, 1000, and 1500 Ω.

https://doi.org/10.1017/S1759078717000952 Published online by Cambridge University Press

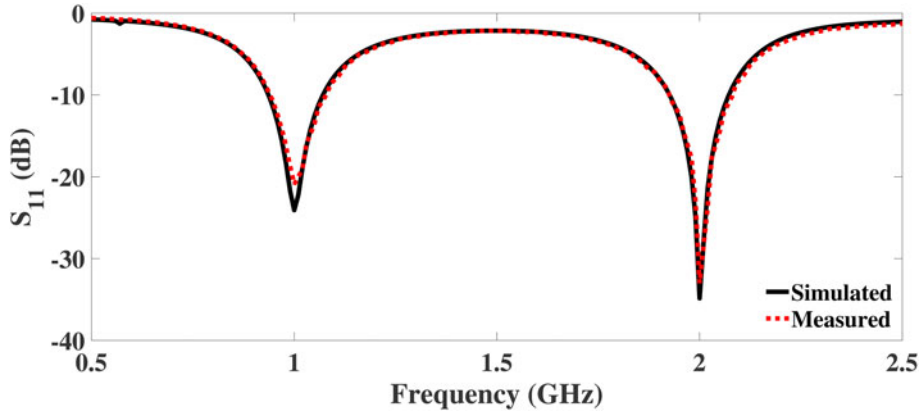

Fig. 10. Simulated and measured return loss of the proposed DBIT for a real load impedance of $Z_L = 500\ \Omega$.

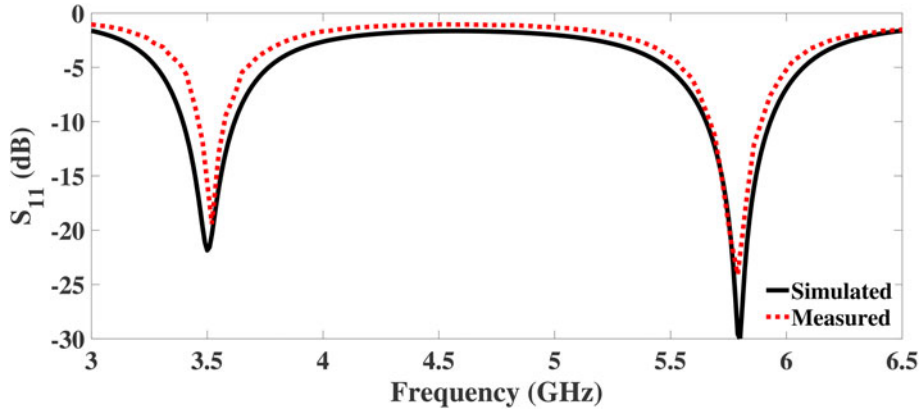

Fig. 11. Simulated and measured return loss of the proposed DBIT for a real load impedance of $Z_L = 1000\ \Omega$.

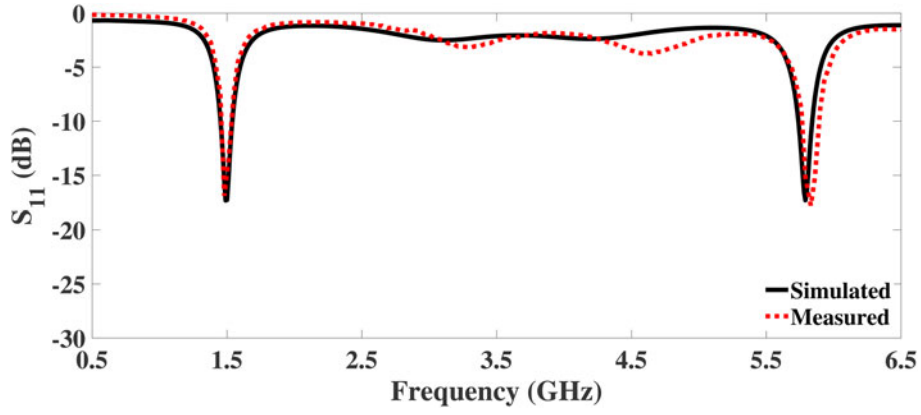

Fig. 12. Simulated and measured return loss of the proposed DBIT for a real load impedance of $Z_L = 1500\ \Omega$.

Table 8. Simulated and measured S_{11} comparison.

	S_{11} (dB)					
	DBIT I		DBIT II		DBIT III	
	@ f_1	@ f_2	@ f_1	@ f_2	@ f_1	@ f_2
Simulated	−24.0	−34.85	−21.85	−30.03	−17.28	−16.59
Measured	−20.9	−33.0	−16.5	−22.5	−15.4	−16.0

Table 9. Simulated and measured bandwidth comparison.

	Bandwidth (in MHz)					
	DBIT I		DBIT II		DBIT III	
	@ f_1	@ f_2	@ f_1	@ f_2	@ f_1	@ f_2
Simulated	134	140	210	270	85	100
Measured	130	150	100	210	85	100

https://doi.org/10.1017/S1759078717000952 Published online by Cambridge University Press

Table 10. Comparison of impedance transforming ratios with previous reported works.

Ref	Techniques	Frequency of operation	Z_L/Z_o
[10]	π-type	Dual-band	4.3*
[11]	Two line-section	Dual-band	3.7*
[12]	Two-section transformer	Dual-band	3.7*
[13]	Two-section transformer	Dual-band	3.7*
[14]	Chebyshev transformer	Dual-band	3.7*
[17]	Coupled-line section	Single-band	3.4†
[18]	Coupled three-line structure	Single-band	3.4†
[19]	Modified coupled line structure	Single-band	5†
[20]	Modified 4:1 Guanella IT	Single-band	5†
[21]	Coupled-line and shunt stub	Single-band	5†
[22]	Open-circuited coupled lines	Single-band	10†
[23]	Multi-section coupled lines	Single-band	20†
This work	Transmission-line and short-ended stubs	Dual-band	10, 20, and 30
		Tri-band	10

*Transforming ratio is calculated based on the design equations presented in [10–14].
†Wideband impedance transformer.

the parameter values, the physical dimensions are calculated and depicted in Table 7. The proposed DBIT is fabricated on a low cost 0.8 thick FR4 epoxy substrate having dielectric constant 4.4, and loss tangent 0.019. The photograph of the fabricated DBITs are shown in Fig. 9. The circuit areas of the DBIT I, II, and III are 57.9×58.1 mm^2, 19.2×18 mm^2, and 46.68×25.9 mm^2, respectively.

R & S ZVL vector network analyzer is used to test the fabricated DBITs. Figures 10–12 illustrate the comparison of simulated and measured return loss (S_{11}) of the DBIT I, II, and III, respectively. The S_{11} is better than 15 dB at each operating frequency for all the fabricated devices. From the plots, it is revealed that the proposed DBITs provide excellent matching between the load impedances ($Z_L = 500$, 1000, and 1500 Ω) and source impedance of 50 Ω at all operating frequencies. The exact values of the S_{11} and bandwidth of the fabricated prototypes are illustrated in Tables 8 and 9, respectively. Comparison of the proposed work with current state of art in terms of impedance transforming ratios and frequency bands is summarized in Table 10.

VII. CONCLUSION

A new dual-band topology is proposed to design a ultra-high transforming IT. A detailed analysis has been worked out to provide exact closed form solution. Based on the derived equations, two examples of dual-band transformer working at smaller and larger frequency ratios are designed for different load impedances. Finally, three prototypes of DBIT with various transforming ratios are fabricated and verified. The measured S_{11} is >15 dB at each frequency band. The tested results show excellent agreement with the simulated results. In addition to dual-band operation, we explored the multi-band characteristic of the proposed network and designed a tri-band transformer for a transforming ratio of 10. The proposed dual-frequency structure is also employed to match a complex load. Hence, the multi-band characteristic of the presented matching network is suitable in the design of multi-frequency power amplifiers, low noise amplifiers, rectification circuits, etc.

REFERENCES

[1] Sun, H.; Guo, Y.X.; He, M.; Zhong, Z.: A dual-band rectenna using broadband Yagi antenna array for ambient RF power harvesting. IEEE Antennas Wireless. Propag. Lett., **12** (2013), 918–921.

[2] Yang, X.X.; Jiang, C.; Elsherbeni, A.Z.; Yang, F.; Wang, Y.Q.: A novel compact printed rectenna for data communication systems. IEEE Trans. Antennas Propag., **61** (2013), 2532–2539.

[3] Chuang, M.L.: Dual-band impedance transformer using two-section shunt stubs. IEEE Trans. Microw. Theory Tech., **58** (2010), 1257–1263.

[4] Nikravan, M.A.; Atlasbaf, Z.: T-section dual-band impedance transformer for frequency-dependent complex impedance loads. Electron. Lett., **47** (2011), 551–553.

[5] Manoochehri, O.; Asoodeh, A.; Forooraghi, K.: Pi -model dual-band impedance transformer for unequal complex impedance loads. IEEE Microw. Wireless Compon. Lett., **25** (2015), 238–240.

[6] Barik, R.K.; Bishoyi, P.K.; Karthikeyan, S.S.: Design of a novel dual-band impedance transformer, in Proc. IEEE Int. Conf. on Electronics, Computing and Communication Technologies (CONECCT), 2015, 1–4.

[7] Chuang, M.L.; Wu, M.T.: General dual-band impedance transformer with a selectable transmission zero. IEEE Trans. Compon. Packag. Manuf. Technol., **6** (2016), 1113–1119.

[8] Barik, R.K.; Siddiqui, R.; Kumar, K.V.P.; Karthikeyan, S.S.: Design of a novel dual-band low noise amplifier incorporating dual-band impedance transformer, in Proc. Int. Conf. on Signal Processing and Communications (SPCOM), 2016, 1–5.

[9] Maktoomi, M.A.; Hashmi, M.S.; Ghannouchi, F.M.: Improving load range of dual-band impedance matching networks using load-healing concept. IEEE Trans. Circuits Syst. II: Express Briefs, **64** (2017), 126–130.

[10] Rawat, K.; Ghannouchi, F.M.: Dual-band matching technique based on dual-characteristic impedance transformers for dual-band power amplifiers design. IET Microw. Antennas Propag., **5** (2011), 1720–1729.

[11] Chow, Y.L.; Wan, K.L.: A transformer of one-third wavelength in two sections - for a frequency and its first harmonic. IEEE Microw. Wireless Compon. Lett., **12** (2002), 22–23.

https://doi.org/10.1017/S1759078717000952 Published online by Cambridge University Press

[12] Monzon, C.: Analytical derivation of a two-section impedance transformer for a frequency and its first harmonic. IEEE Microw. Wireless Compon. Lett., **12** (2002), 381–382.

[13] Monzon, C.: A small dual-frequency transformer in two sections. IEEE Trans. Microw. Theory Tech., **51** (2003), 1157–1161.

[14] Orfanidis, S.J.: A two-section dual-band Chebyshev impedance transformer. IEEE Microw. Wireless Compon. Lett., **13** (2003), 382–384.

[15] Wang, X.; Ohira, M.; Ma, Z.: A flexible two-section transmission-line transformer design approach for complex source and real load impedances. IEICE Electron. Express, **14** (2017), 20161095–20161095.

[16] Wang, X.; Ma, Z.; Sakagami, I.; Mase, A.; Yoshikawa, M.: Small, single-band, two-section transformer for real load impedances with symmetry property. Electron. Lett., **52** (2016), 934–936.

[17] Nguyen, H.T.; Ang, K.S.; Ng, G.I.: Design of coupled three-line impedance transformers. IEEE Microw. Wireless Compon. Lett., **24** (2014), 84–86.

[18] Ang, K.S.; Lee, C.H.; Leong, Y.C.: Analysis and design of coupled line impedance transformers, in IEEE MTT-S Int. Microwave Symp. Digest, vol. **3**, 2004, 1951–1954.

[19] Chen, M.G.; Hou, T.B.; Tang, C.W.: Design of planar complex impedance transformers with the modified coupled line. IEEE Trans. Compon. Packag. Manuf. Technol., **2** (2012), 1704–1710.

[20] Ehsan, N.; Hsieh, W.T.; Moseley, S.H.; Wollack, E.J.: Broadband planar 5:1 impedance transformer. IEEE Microw. Wireless Compon. Lett., **25** (2015), 636–638.

[21] Kim, P.; Chaudhary, G.; Jeong, Y.: Enhancement impedance transforming ratios of coupled line impedance transformer with wide out-of-band suppression characteristics. Microw. Opt. Technol. Lett., **57** (2015), 1600–1603.

[22] Kim, P.; Chaudhary, G.; Jeong, Y.: Ultra-high transforming ratio coupled line impedance transformer with bandpass response. IEEE Microw. Wireless Compon. Lett., **25** (2015), 445–447.

[23] Wu, Q.S.; Zhu, L.: Short-ended coupled-line impedance transformers with ultrahigh transforming ratio and bandpass selectivity suitable for large load impedances. IEEE Trans. Compon. Packag. Manuf. Technol., **6** (2016), 767–774.

[24] Barik, R.K.; Karthikeyan, S.S.: A novel quad-band impedance transformer with ultra-high transforming ratio. Int. J. Electron. Commun., **78** (2017), 157–161.

[25] Barik, R.K.; Karthikeyan, S.S.: A novel design of ultra-high impedance transforming ratio quad-band matching network. Microw. Opt. Technol. Lett., **59** (2017), 2021–2026.

[26] Pozar, D.M.: Microwave Engineering, Wiley, New York, 2005.

Rusan Kumar Barik was born in Odisha, India. He received the B. Tech degree in Electronics and Tele-Communication Engineering from Biju Patnaik University of Technology, Rourkela, India in 2012 and the M. Des degree in Communication Systems Design from Indian Institute of Information Technology Design and Manufacturing, Kancheepuram, India in 2015, where he is currently working towards his Ph.D. degree. His research interests include design of multi-band microwave passive components and low noise amplifier for millimeter wave applications.

S. S. Karthikeyan was born in Mayiladuthurai, Tamilnadu, India. He received the B.E. degree in Electronics and Communication Engineering from Bharathidasan University, Trichy, in 2001 and M.E. in Applied Electronics from Sathyabama University, Chennai, in 2005. He obtained his Doctoral Degree from the Indian Institute of Technology Guwahati, Assam, India in 2011. Currently he is working as an Assistant Professor at the Indian Institute of Information Technology, Design and Manufacturing Kancheepuram, Chennai, India. His research interests include electromagnetic bandgap substrates, microwave filters, metamaterials, microwave sensors, etc.

https://doi.org/10.1017/S1759078717000952 Published online by Cambridge University Press